Inorg. Chem. **2005**, *44*, 7214–7225

Copper(II) Interaction with Unstructured Prion Domain Outside the Octarepeat Region: Speciation, Stability, and Binding Details of Copper(II) Complexes with PrP106–126 Peptides

Giuseppe Di Natale,[†] Giulia Grasso,[‡] Giuseppe Impellizzeri,[†] Diego La Mendola,[‡] Giovanni Micera,[§] Nikolett Mihala,[||] Zoltán Nagy,[⊥] Katalin Õsz,[⊥] Giuseppe Pappalardo,[‡] Viktória Rigó,[⊥] Enrico Rizzarelli,*[,†,‡] Daniele Sanna,[#] and Imre Sóvágó*[,⊥]

Dipartimento di Scienze Chimiche, Università di Catania, V.le A. Doria 6, 95125 Catania, Italy, Istituto di Biostrutture e Bioimmagini-Sezione di Catania, CNR, V.le A. Doria 6, 95125 Catania, Italy, Dipartimento di Chimica, Università di Sassari, Via Vienna 2, 07100 Sassari, Italy, Research Group of Peptide Chemistry, Hungarian Academy of Sciences, H-1518 Budapest, Hungary, Department of Inorganic and Analytical Chemistry, University of Debrecen, H-4010 Debrecen, Hungary, and Istituto di Chimica Biomolecolare-Sezione di Sassari, CNR, Traversa La Crucca 3, Regione Baldinca, 07040 Li Punti (SS), Italy

Received May 12, 2005

Copper(II) complexes of the neurotoxic peptide fragments of human and chicken prion proteins were studied by potentiometric, UV–vis, CD, and EPR spectroscopic and ESI-MS methods. The peptides included the terminally blocked native and scrambled sequences of HuPrP106–126 (HuPrPAc106–126NH_2 and ScrHuPrPAc106–126NH_2) and also the nona- and tetrapeptide fragments of both the human and chicken prion proteins (HuPrPAc106–114NH_2, ChPrPAc119–127NH_2, HuPrPAc109–112NH_2, and ChPrPAc122–125NH_2). The histidyl imidazole-N donor atoms were found to be the major copper(II) binding sites of all peptides; 3N and 4N complexes containing additional 2 and 3 deprotonated amide-N donors, respectively, are the major species in the physiological pH range. The complex formation processes for nona- and tetrapeptides are very similar, supporting the fact that successive deprotonation and metal ion coordination of amide functions go toward the N-termini in the form of joined six- and five-membered chelates. As a consequence, the peptide sequences investigated here, related to the neurotoxic region of the human PrP106–126 sequence, show a higher metal-binding affinity than the octarepeat fragments. In the case of the HuPrP peptide sequences, a weak pH-dependent binding of the Met109 residue was also detected in the 3N-coordinated complexes.

Introduction

Prion diseases are neurodegenerative disorders associated with a conformational change in the normal cellular isoform of the prion protein, PrP^C, to an abnormal scrapie isoform, PrP^{Sc}.[1,2]

Unlike the α-helical PrP^c, the protease-resistant core of PrP^{sc} has a predominantly β-sheet form and possesses a tendency to polymerize into amyloid fibrils.[3,4] These rod-shaped fibrils accumulate in the nervous system giving rise to protein depositions or plaques, often associated with neuronal death[5] through the triggering of the apoptotic program[6] and astrogliosis.[7]

Unfortunately, structural studies of the pathogenic form have been hampered by the insolubility, heterogeneity, and complexity of the PrP^{Sc} isoforms. Thus, synthetic peptides

* To whom correspondence should be addressed. E-mail: erizzarelli@unict.it (E.R.); sovago@delfin.unideb.hu (I.S.).
[†] Università di Catania.
[‡] Istituto di Biostrutture e Bioimmagini-Sezione di Catania.
[§] Università di Sassari.
[||] Hungarian Academy of Sciences.
[⊥] University of Debrecen.
[#] Istituto di Chimica Biomolecolare-Sezione di Sassari.

(1) Prusiner, S. B. *Science* **1982**, *216*, 136−144.
(2) Prusiner, S. B.; De Armond, S. J. *Annu. Rev. Neurosci.* **1994**, *17*, 311−339.
(3) Prusiner, S. B.; McKinley, M. P.; Bowman, K. A.; Bolton, D. C.; Bondheim, P. E.; Groth, D. F.; Glenner, G. G. *Cell* **1983**, *35*, 349−358.
(4) Pern, K.; Baldwin, M.; Nguyen, J.; Gasset, M.; Serban, A.; Groth, D.; Mehlhorn, I.; Huang, Z.; Fletterick, R. J.; Cohen F. E.; Prusiner S. B. *Proc. Natl. Acad. Sci. U.S.A.* **1993**, *90*, 10962−10966.

10.1021/ic050754k CCC: $30.25
Published on Web 08/31/2005

derived from discrete PrP regions have been used extensively to identify the protein domains that could be involved in the conformational transition from PrP^C to PrP^{Sc} and in disease pathogenesis.[8] Previous studies have shown that a synthetic peptide encompassing human PrP residues 106−126 exhibits some of the pathogenic and physicochemical properties of PrP^{Sc}.[9] PrP106−126 is highly conserved among various species, and it has been suggested to represent one of the key domains where conformational changes initiate, leading to the conversion of PrP^C to PrP^{Sc}.[10−13]

This protein fragment is both highly fibrillogenic and toxic to neurons in vitro, requiring PrP^C expression for neurotoxicity.[14,15] In particular, the palindrome region AGAAAAGA, encompassing residues 113−120 of PrP106−126, has been shown to be necessary for both fibril formation and PrP^{Sc}-like toxicity.[16,17] Further studies brought into evidence that His111 plays a central role in the structural features of this peptide; in addition, the amidation of the C-terminus has been shown to drive the peptide toward a predominant random-coil conformation, decreasing the tendency to generate amyloid fibrils.[18] The environment (pH, metal ions, lipid membranes, etc.) induces a remarkable conformational polymorphism on PrP106−126, which acquires different secondary structures. The capacity of bathocuproin sulfonate to abolish the neurotoxicity of PrP106−126 has recently suggested the involvement of copper(II) in the activity of the peptide.[19] The link between copper(II) binding to PrP106−126 and peptide toxicity has also been proved by the involvement of the metal ion in copper(II)-mediated hydrogen peroxide generation[20] and by the role of copper-(II) in modulating the ability of PrP106−126 to form an ion channel.[21,22] It has also been found that the interaction of Cu/Zn with the His111 residue of PrP106−126 induces fibrillogenesis.[23] In that report, the metal complex species responsible for the aggregation process were not identified, casting a shadow on the coordination model proposed.[23] Previous investigations have been carried out on copper(II) complexes with PrP106−126 and its polar fragment PrP106−114 with the N- and C-termini blocked; the results allowed us to determine the stoichiometry of the complex species and, in contrast with previous investigations,[23] to show that the N-termini acetylated peptides are able to bind copper-(II).[24,25] A thermodynamic study of copper (II) complexes with the amidate form of PrP106−113 and unblocked C- and N-termini of PrP106−126 peptides has recently been reported.[26] However, these prion protein fragments may not represent reliable models for this unstructured region of the whole PrP^C protein, as very recently stressed.[27] Conversely, blocking both the N- and C-termini in these peptide fragments, while avoiding trivial metal interaction with the terminal amino and carboxyl groups, results in a better reproduction of the conditions present in the full-length native protein.

Chart 1. Prion Peptide Fragments Investigated

$HuPrPAc106\text{-}126NH_2$	Ac-KTNMKHMAGAAAAGAVVGGLG-NH_2
$HuPrPAc106\text{-}114NH_2$	Ac-KTNMKHMAG-NH_2
$ChPrPAc119\text{-}127NH_2$	Ac-KTNFKHVAG-NH_2
$ChPrPAc122\text{-}125NH_2$	Ac-FKHV-NH_2
$HuPrPAc109\text{-}112NH_2$	Ac-MKHM-NH_2
$ScrPrPAc106\text{-}126NH_2$	Ac-NGAKALMGGHGATKVMVGAAA-NH_2

In the present study, we report the characterization of the copper(II) complex species formed with the PrP106−126 peptide bearing both C- and N-termini protected by acetylation and amidation, respectively ($HuPrPAc106\text{−}126NH_2$). In addition, to unambiguously identify the key residues involved in metal coordination, we resorted to a comparative study by synthesising suitable peptide analogues ($HuPrPAc106\text{−}114NH_2$, $ChPrPAc119\text{−}127NH_2$, $HuPrPAc109\text{−}112NH_2$ $ChPrPAc122\text{−}125NH_2$) related to human or chicken sequences (Chart 1) and investigating their complexing properties. The chicken prion protein (ChPrP) shares some

(5) Bruce, M. E.; McBride, P. A.; Farguhar, G. F. *Neurosci. Lett.* **1989**, *102*, 1−6.
(6) Gray, F.; Chretien, F.; Biassette, H. A.; Doranden, A.; Ereau, T.; Delisle, M. B.; Kopp, N.; Ironside, J. W.; Vital, C. *J. Neuropathol. Exp. Neural.* **1999**, *58*, 321−328.
(7) De Armond, S. J.; Gonzales, M.; Mobley, W. C.; Kon, A. A.; Stern, A.; Prusiner, H.; Prusiner, S. B. *Prog. Clin. Biol. Res.* **1989**, *317*, 601−618.
(8) Tagliavini, F.; Forloni, G.; D'Ursi, P.; Bugiani, O.; Salmona, M. *Adv. Protein Chem.* **2001**, *57*, 171−201.
(9) Forloni, G.; Angeretti, N.; Chiesa, R.; Monzani, E.; Salmona, M.; Bugiani, O.; Tagliavini, F. *Nature* **1993**, *362*, 543−546.
(10) Muramoto, T.; Scott, M.; Cohen, F. E.; Prusiner, S. B. *Proc. Natl. Acad. Sci. U.S.A.* **1996**, *93*, 15457−15462.
(11) Fisher, M.; Rulicke, T.; Raeber, A.; Sailer, A.; Moser, M.; Oesch, B.; Brandner, S.; Aguzzi, A.; Weissmann, C. *EMBO J.* **1996**, *15*, 1255−1264.
(12) Muramoto, T.; DeArmond, S. J.; Scott, M.; Telling, G. C.; Cohen, F. E.; Prusiner, S. B. *Nat. Med.* **1997**, *3*, 750−755.
(13) Brown, D. R.; Schmidt, B.; Kretzschamer, H. A. *Nature* **1996**, *380*, 345−347.
(14) Brown, D. R.; Herms, J.; Kretzschmar, H. A. *NeuroReport* **1994**, *5*, 2057−2060.
(15) Hope, J.; Shearman, M. S.; Baxter, H. C.; Chong, A.; Kelly, S. M.; Price, N. C. *Neurodegeneration* **1996**, *5*, 1−11.
(16) Brown, D. R. *Mol. Cell Neurosci.* **2000**, *15*, 66−78.
(17) Jobling, M. F.; Stewart, L. R.; White, A. R.; McLean, C.; Friedhuber, A.; Maher, F.; Beyrenther, K.; Masters, C. L.; Barrow, C. J.; Collins, S. J.; Cappai, R. *J. Neurochem.* **1999**, *73*, 1557−1565.
(18) Salmona, M.; Malesani, P.; De Gioia, L.; Gorla, S.; Bruschi, M.; Molinari, A.; Della Vedova, F.; Pedrotti, B.; Marrani, M. A.; Awans, T.; Bugiani, O.; Forloni, G.; Tagliavini, F. *Biochem. J.* **1999**, *342*, 207−214.
(19) Brown, D. R. *Biochem. J.* **2000**, *352*, 511−518.
(20) Turnbull, S.; Tabner, B. J.; Brown, D. R.; Allsop, D. *Neurosci. Lett.* **2003**, *336*, 159−162.
(21) Kourie, J. I.; Farrelly, P. V.; Henry, C. L. *J. Neurosci. Res.* **2001**, *66*, 214−220.
(22) Kourie, J. I.; Kenna, B. L.; Tew, D.; Jobling, M. F.; Curtain, C. C.; Masters, C. L.; Barnham, K. J.; Cappai, R. *J. Membrane Biol.* **2003**, *193*, 35−45.
(23) Jobling, M. F.; Huang, X.; Stewart, L. R.; Barnham, K. J.; Curtain, C.; Volitakis, I.; Perugini, M.; White, A. R.; Cherny, R. A.; Masters, C. L.; Barrow, C. J.; Collins, S. J.; Bush, A. I.; Cappai, R. *Biochemistry* **2001**, *40*, 8073−8084.
(24) Pappalardo, G.; Campagna, T.; Grasso, G.; Impellizzeri, G.; Rizzarelli, E. In *Peptides 2002*; Benedetti, E., Pedone, C., Eds.; Ziino: Naples, 2002; pp 840−841.
(25) Bonomo, R. P.; Grasso, D.; Grasso, G.; Guantieri, V.; Impellizzeri, G.; La Rosa, C.; Milardi, D.; Pappalardo, G.; Tabbì, G.; Rizzarelli, E. In *Metal Ligand Interactions in Molecular-, Nano-, Micro- and Macro-Systems in Complex Environments*; Russo, N., Salahub, D. R., Witko, M., Eds.; Kluwer Academic Publishers: Dordrecht, The Netherlands, 2003; pp 19−36.
(26) Belosi, B.; Gaggelli, E.; Guerrini, R.; Kozlowski, H.; Luczkowski, M.; Mancini, F. M.; Remelli, M.; Valensin, D.; Valensin, G. *Chembiochem* **2004**, *5*, 349−359.
(27) Jones, C. E.; Abdelraheim, S. R.; Brown, D. R.; Viles, J. H. *J. Biol. Chem.* **2004**, *279*, 32018−32027.

essential features with the human one, despite low sequence homology; in particular, the unstructured region outside the N-terminus domain is almost perfectly retained with the exception of the two methionine residues (109 and 112 positions in HuPrP), which are replaced by a phenylalanine and valine residues, respectively (122 and 125 positions in ChPrP). We used potentiometric and spectroscopic techniques (UV−vis, CD, and EPR) to study the speciation, affinity, folding, and bonding details of copper(II) complexes with the PrP peptide fragments investigated. Only in the case of the HuPrPAc106−126NH_2, because of the low solubility of this peptide and of its metal complexes, the stoichiometry of the copper(II) complexes was determined by means of ESI-MS. Finally, the comparison of the results with those obtained with a scrambled analogue ScrHuPrPAc106−126NH_2 (Chart 1) allowed us to ascertain a sequence-specific behavior of the coordinated metal ion.

Three different regions of PrP^c have been indicated as binding sites for the copper(II): i) the octarepeat domain,[25,28−30] (ii) the unstructured region encompassing the 91−115 residues,[27,31,32] and (iii) helix 2 of the structured C-terminus.[33−35] Stability constant values have been reported for mono-, bis-, and tetra-octarepeat complexes of copper(II).[36] The results concerning the copper(II) complexes with HuPrPAc106−126NH_2 and the related fragments, here reported, now allow a reliable comparison between the metal ion affinity of the two binding sites located within the disordered region, showing also the coordination features of the main species formed in the physiological pH range.

Experimental Section

General. All *N*-fluorenylmethoxycarbonyl (Fmoc)-protected amino acids (Fmoc-Lys(Boc)-OH, Fmoc-Thr(tBu)-OH, Fmoc-Asn(Trt)-OH, Fmoc-Met-OH, Fmoc-His(Trt)-OH, Fmoc-Ala-OH, Fmoc-Val-OH, Fmoc-Leu-OH, Fmoc-Gly-OH and Fmoc-Phe-OH) and 2-(1-H-benzotriazole-1-yl)-1,1,3,3-tetramethyluronium tetrafluoroborate (TBTU) were obtained from Novabiochem (Switzerland); Fmoc PAL-PEG resin, *N*,*N*-diisopropyl-ethylamine (DIEA), *N*,*N*-dimethylformamide (DMF, peptide synthesis grade), and a 20% piperidine−DMF solution were obtained from Applied Biosystems. *N*-hydroxybenzotriazole (HOBT), triisopropylsilane (TIS), trifluoroacetic acid (TFA), and ethandithiol (EDT) were purchased from Sigma/Aldrich. All other chemicals were of the highest available grade and were used without further purification.

Preparative reversed-phase high-performance liquid chromatography (rp-HPLC) was carried out using a Varian PrepStar 200 model SD-1 chromatography system equipped with a Prostar photodiode array detector with detection at 222 nm. Purification was performed by eluting with solvents A (0.1% TFA in water) and B (0.1% TFA in acetonitrile) on a Vydac C_{18} 250 × 22 mm (300 Å pore size, 10−15 μm particle size) column, at flow rate of 10 mL/min. Analytical rp-HPLC analyses were performed using a Waters 1525 instrument equipped with a Waters 2996 photodiode array detector with detection at 222 nm.

The peptide samples were analyzed using gradient elution with solvents A and B on a Vydac C_{18} 250 × 4.6 mm (300 Å pore size, 5 μm particle size) column, run at a flow rate of 1 mL/min.

Peptide Synthesis and Purification. The synthesis of HuPrPAc106−126NH_2 and HuPrPAc106−114NH_2 was reported elsewhere.[37]

The scrambled ScrHuPrPAc106−126NH_2, the ChPrPAc119−127NH_2, the ChPrPAc122−125NH_2, and the HuPrPAc109−112NH_2 peptides were assembled using the solid-phase peptide synthesis strategy on a Pioneer Peptide Synthesizer. All residues were introduced according to the TBTU/HOBT/DIEA activation method for Fmoc chemistry on Fmoc-PAL-PEG resin (substitution 0.22 mmol/g, 0.33 mmol scale synthesis, 1.5 g of resin). The synthesis was carried out under a 4-fold excess of amino acid at every cycle and each amino acid was recirculated through the resin for 35 min. Fmoc protection was removed during synthesis with a 20% piperidine solution in DMF. N-terminal acetylation was performed by treating the fully assembled and protected peptide resins (after removal of the N-terminal Fmoc group) with a solution containing acetic anhydride (6% v/v) and DIEA (5% v/v) in DMF.

The peptides were cleaved from their respective resins and simultaneously deprotected by treatment with a mixture of TFA/TIS/H_2O (95/2.5/2.5 v/v) for 2 h at room temperature. Each solution containing the free peptide was separated from the resin by filtration and concentrated in vacuo at 30 °C. The peptide was precipitated with cold freshly distilled diethyl ether. The precipitate was then filtered, dried under vacuum, redissolved in water, and lyophilised. The resulting crude peptides were purified by preparative rp-HPLC.

Ac-NGAKALMGGHGATKVMVGAAA-NH_2 (ScrHuPrPAc106−126NH_2). Linear gradient: 0 to 25% B over 35 min. Yield: 36% [R_t = 20.23 min]. Analytical rp-HPLC: 15 to 25% B over 20 min [R_t = 17.04 min]. ESI-MS obsd *m*/*z*: $(M + H)^+$ 1953.5, $(M + 2H)^{2+}$ 977.2, $(M + 3H)^{3+}$ 651.9. Calcd for $C_{82}H_{141}N_{27}O_{24}S_2$: 1952.00.

Ac-KTNFKHVAG-NH_2 (ChPrPAc119−127NH_2). Linear gradient: 0 to 15% B over 45 min. Yield: 60% [R_t = 29.70 min]. Analytical rp-HPLC: 5 to 15% B over 25 min [R_t = 21.00 min]. ESI-MS obsd *m*/*z*: $(M + H)^+$ 1042.50, $(M + 2H)^{2+}$ 522.30, $(M + 3H)^{3+}$ 348.10. Calcd for $C_{47}H_{75}N_{15}O_{12}$: 1041.57.

Ac-FKHV-NH_2 (ChPrPAc122−125NH_2). Linear gradient: 10 to 35% B over 30 min. Yield: 60% [R_t = 26.00 min]. Analytical rp-HPLC: 5 to 15% B over 20 min [R_t = 19.00 min]. ESI-MS obsd *m*/*z*: $(M + H)^+$ 571.49. Calcd for $C_{28}H_{42}N_8O_5$: 570.33.

Ac-MKHM-NH_2 (HuPrPAc109−112-NH_2). Linear gradient: 5 to 25% B over 25 min. Yield: 75% [R_t = 23.00]. Analytical rp-HPLC: 5 to 15% B over 20 min [R_t = 16.10 min]. ESI-MS obsd *m*/*z*: $(M + H)^+$ 587.70. Calcd for $C_{24}H_{42}N_8O_5S_2$: 586.27.

(28) Viles, J. H.; Cohen, F. E.; Prusiner, S. B.; Goodin, D. B.; Wright, P. E.; Dyson, J. H. *Proc. Natl. Acad. Sci. U.S.A.* **1999**, *96*, 2042−2047.
(29) Bonomo, R. P.; Cucinotta, V.; Giuffrida, A.; Impellizzeri, G.; Magrì, A.; Pappalardo, G.; Rizzarelli, E.; Santoro, A. M.; Tabbì, G.; Vagliasindi, L. *Dalton Trans.* **2005**, 150−158.
(30) Brown, D. R.; Qin, K.; Herms, J. W.; Madlung, A.; Manson, J.; Strome, R.; Fraser, P. E.; Kruck, T.; von Bohlen, A.; Schulz-Schaeffer, W.; Giese, A.; Westaway, D.; Kretzschmar, H. *Nature* **1997**, *390*, 684−687.
(31) Kramer, M. L.; Kratzin, H. D.; Schimdt, B.; Romer, A.; Windl, O.; Liemann, S.; Hornemann, S.; Kretschmar, H. *J. Biol. Chem.* **2001**, *276*, 16711−16719.
(32) Jackson, G. S.; Murray, I.; Hosszu, L. L.; Gibbs, N.; Waltho, J. P.; Clarke, A. R.; Collinge, J. *Proc. Natl. Acad. Sci. U.S.A.* **2001**, *98*, 8531−8535.
(33) Van Doorslaer, S.; Cereghetti, G. M.; Glockshuber, R.; Schweiger, A. *J. Phys. Chem. B* **2001**, *105*, 1631−1639.
(34) Cereghetti, G. M.; Schweiger, A.; Glockshuber, R.; Van Doorslaer, S. *Biophys. J.* **2003**, *84*, 1985−1997.
(35) Brown, D. R.; Guantieri, V.; Grasso, G.; Impellizzeri, G.; Pappalardo, G.; Rizzarelli, E. *J. Inorg. Biochem.* **2004**, *98*, 133−143.
(36) Valensin, D.; Luczkowski, M.; Mancini, F. M.; Legowska, A.; Gaggelli, E.; Valensin, G.; Rolka, K.; Kozlowski, H. *Dalton Trans.* **2004**, 1284−1293.
(37) Di Natale, G.; Impellizzeri, G.; Pappalardo, G. *Org. Biomol. Chem.* **2005**, *3*, 490−497.

Potentiometric Measurements. The pH-potentiometric titrations were performed in 3−5 cm^3 samples in the concentration range of 2×10^{-3}−4×10^{-3} mol dm^{-3} with metal ion-to-ligand ratios between 1:2 and 2:1. The ScrHuPrPAc106−126NH_2 peptide with the scrambled sequence was soluble under acidic conditions, but precipitation started around pH 7 following the deprotonation of the imidazolium group. Thus, the p*K* values of this ligand were obtained in diluted samples (10^{-4} mol dm^{-3}), and the standard deviation of the equlibrium data is significantly higher than those of the other peptides. Copper(II) complexes of the scrambled peptide were soluble at all pH values, and the millimolar concentration range was used in all measurements. During the titration, argon was bubbled through the samples to ensure the absence of oxygen and carbon dioxide and, also, to stir the solutions. All pH-potentiometric measurements were carried out at 298 K at a constant ionic strength of 0.2 mol dm^{-3} KCl with a Radiometer pHM84 pH-meter equipped with a 6.0234.100 combination glass electrode (Metrohm) and a Dosimat 715 automatic buret (Metrohm) containing carbonate-free potassium hydroxide in known concentration. The pH readings were converted into the hydrogen ion concentration, and the protonation constants of the ligands and the overall stability constants (log β_{pqr}) of the systems were calculated by means of a general computational program, PSEQUAD,[38] using eqs 1 and 2.

$$pM + qH + rL = M_pH_qL_r \quad (1)$$

$$\beta_{pqr} = \frac{[M_pH_qL_r]}{[M]^p[H]^q[L]^r} \quad (2)$$

Spectroscopic Measurements. UV−vis spectra of the copper(II) complexes were recorded on a Hewlett-Packard HP 8453 diode array spectrophotometer in the same concentration range as used for pH-potentiometry. The CD spectra of the copper(II) complexes were recorded on a JASCO J-810 spectropolarimeter using 1 or 10 mm cells in the 200−800 nm range in the same concentration range as used for potentiometry. The UV−vis and CD spectra of the individual species were calculated by the same general program (PSEQUAD) as used for the evaluation of potentiometric measurements.

Frozen-solution EPR spectra were recorded on a Bruker ER 200D spectrometer equipped with the 3220 data system at 150 K. Copper(II) complex solutions (1×10^{-3} mol dm^{-3}) were prepared in situ by mixing the necessary volume of a standard solution of $^{63}Cu(NO_3)_2$ with solutions of the peptide ligands in a 1:1.1 metal-to-ligand ratio and adjusting the pH of the resulting solution to the desired value by adding 1×10^{-2} mol dm^{-3} KOH or HNO_3. Methanol, ca. 10%, was added to the aqueous copper(II) complex solutions to increase resolution.

Electrospray Ionization Mass Spectrometry (ESI-MS) Analysis. ESI-MS spectra were recorded on a Finnigan LCQ-Duo ion trap electrospray mass spectrometer. Peptide solutions were introduced into the ESI source via 100 μm i.d. fused silica from a 250 μl syringe. The experimental conditions for spectra acquired in positive-ion mode were as follows: needle voltage, 2.5 kV; flow rate, 5 μl/min; source temperature, 150 °C; *m*/*z* range, 200−2000; cone potential, 46 V; tube lens offset, 16 V.

The metal complex solutions were prepared by dissolving the peptide and $CuSO_4$ in Milli-Q water at 1:1 ligand-to-metal ratio (ligand concentration ranging from 1×10^{-5} to 5×10^{-5} mol dm^{-3}) and were investigated in the 5.0−9.5 pH range, adjusting the pH values by adding HCl or NaOH.

Because of the isotopic distribution of elements, molecular species were detected as clusters of peaks; to simplify their assignments, the *m*/*z* values indicated in the spectra and in the tables correspond to the first (lowest-mass) peak of each cluster. In the formulas reported in the text and the tables, the substitution of the hydrogen atoms of the peptides with copper atoms is indicated in parentheses: as an example, [(HuPrPAc106−114NH_2, −2H + Cu)]-H^+ indicates a peptide molecule in which two H atoms are substituted by a Cu atom. In all cases, the cationizing agents are placed outside the parentheses and their charge is indicated. Other details are as previously reported.[39,40]

Table 1. Equilibrium Data of the Copper(II) Complexes with the Chicken and Human Peptide Fragments (I = 0.2 mol dm^{-3} KCl, T = 298 K)

species	ChPrPAc-119−127NH_2	HuPrPAc-106−114NH_2	ScrHuPrPAc-106−126NH_2
p*K*(His)	6.22(1)	6.24(1)	6.43(5)
p*K*(Lys_1)	9.89(1)	9.91(1)	9.61(15)
p*K*(Lys_2)	10.62(2)	10.54(2)	10.24(20)
	logβ	logβ	logβ
[CuH_2L]	24.19(2)	23.54(3)	23.52(5)
[CuHL]	−	17.61(9)	−
[CuL]	12.39(2)	12.39(2)	11.75(3)
[$CuH_{-1}L$]	5.34(1)	4.56(1)	4.40(3)
[$CuH_{-2}L$]	−4.65(2)	−5.45(2)	−5.13(4)
[$CuH_{-3}L$]	−15.25(3)	−16.11(3)	−15.51(5)
pK_{-1}	−	5.93	−
pK_{-2}	−	5.22	−
pK_{-12}	5.90	5.58	5.89
pK_{-3}	7.05	7.83	7.35
p*K*(Cu-Lys_1)	9.99	10.01	9.53
p*K*(Cu-Lys_2)	10.60	10.66	10.38

Results and Discussions

Proton and Copper(II) Complexes: Formation and Bonding Details. Protonation constants of the peptide ligands and stability constants of the copper(II) complexes of the HuPrPAc106−114NH_2, ChPrPAc119−127NH_2, and ScrHuPrPAc106−126NH_2 are presented in Table 1.

All of these peptide ligands have three protonation sites: the imidazole nitrogen atom of His and the ϵ-amino groups of two Lys residues. The protonation constants of the imidazole nitrogen atoms of the ligands are very similar to each other, and the values are in good agreement with other histidine-containing fragments of prion proteins.[36,41,42] Deprotonation of the lysyl ammonium groups takes place in the pH range from 9 to 11, and the values are close to those of other lysine-containing peptides.[43]

Copper(II)−peptide systems were investigated at three different metal ion-to-ligand ratios: 1:1, 2:1, and 1:2. The number of base equivalents of titration curves and the computer evaluation of the data, however, indicated that only 1:1 complexes are formed at any metal ion-to-ligand ratios.

(38) Zékány, L.; Nagypál, I. In *Computational Methods for the Determination of Stability Constants*; Leggett, D. J., Ed.; Plenum Press: New York, 1985; p 291.
(39) La Mendola, D.; Mineo, P.; Rizzarelli, E.; Scamporrino, E.; Vecchio, G.; Vitalini, D. *J. Supramol. Chem.* **2001**, *1*, 147−151.
(40) Mineo, P.; Vitalini, D.; La Mendola, D.; Rizzarelli, E.; Scamporrino, E.; Vecchio, G. *Mass. Spectrom. Rapid Commun.* **2002**, *16*, 722−729.
(41) Luczkowski, M.; Kozlowski, H.; Stawikowski, M.; Rolka, K.; Gaggelli, E.; Valensin, D.; Valensin, G. *Dalton Trans*. **2002**, 2269−2274.
(42) Luczkowski, M.; Kozlowski, H.; Legowska, A.; Rolka, K.; Remelli, M. *Dalton Trans*. **2003**, 619−624.
(43) Sóvágó, I.; Bertalan, Cs.; Göbl, L.; Schõn, I.; Nyéki, O. *J. Inorg. Biochem*. **1994**, *55*, 67−75.

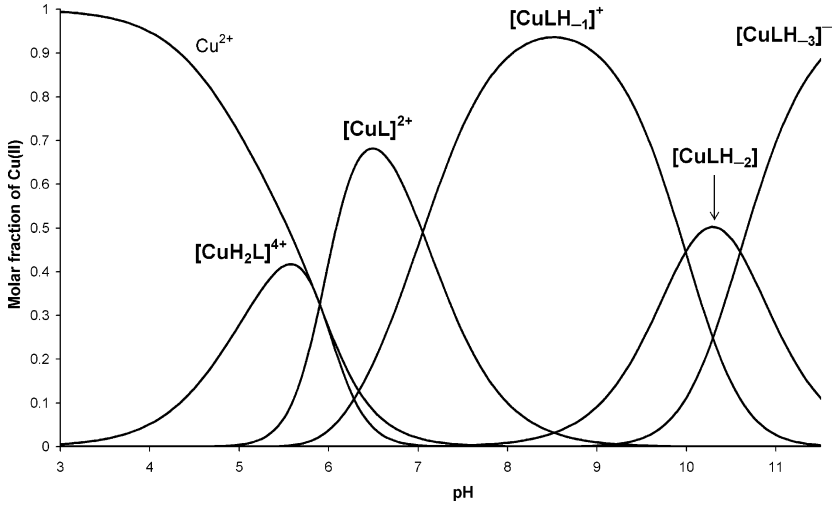

Figure 1. Species distribution diagram for the copper(II)−ChPrPAc119−127NH_2 system (metal-to-ligand ratio 1:1; L = ChPrPAc119−127NH_2). [L] = 2×10^{-3} mol dm^{-3}.

Table 2. Spectroscopic Parameters of the Copper(II) Complexes with the Prion Peptide Fragments

	species	UV−vis $\lambda_{max}(\epsilon)$ [nm($dm^3mol^{-1}cm^{-1}$)]	CD $\lambda_{max}(\Delta\epsilon)$ [nm($dm^3mol^{-1}cm^{-1}$)]	EPR $g_{\|\|}/A_{\|\|}$ (10^{-4} cm^{-1})
ChPrPAc119−127NH_2	[CuH_2L]	772 (28)	−	2.366/135
	[CuL]	610 (72)	615 (−0.19), 525(+0.42)	2.231/169
			350 (−0.77); 248 (+7.21)	
			224 (−7.69)	
	[$CuH_{-1}L$]	538 (117)	645 (+1.27), 500 (−1.35)	2.201/194
	[$CuH_{-2}L$]		325 (+0.97), 293 (−0.75)	
	[$CuH_{-3}L$]		260 (+7.14), 224 (+25.4)	
HuPrPAc106−114NH_2	[CuH_2L]	760 (28)	−	2.366/133
	[CuHL]	−	−	−
	[CuL]	616 (77)	760 (−0.22), 535 (+0.39)	2.220/174
			385 (+0.11), 330 (−0.61)	
			249 (+8.29)	
	[$CuH_{-1}L$]	532 (108)	631 (+1.05), 495 (−1.22)	2.198/198
	[$CuH_{-2}L$]		317 (+1.27), 292 (+0.16)	
	[$CuH_{-3}L$]		256 (+7.82)	
ScrHuPrPAc106−126NH_2	[CuH_2L]	760 (28)	−	2.358/141
	[CuHL]	−	−	−
	[CuL]	610 (79)	328 (+0.68), 225 (−9.20)	2.232/173
	[$CuH_{-1}L$]	550 (125)	600 (−0.32), 505 (+1.05)	2.201/195
	[$CuH_{-2}L$]		305 (−0.75), 247 (+1.00)	
	[$CuH_{-3}L$]		229 (−1.40)	

The metal ion speciations of the three systems are very similar to each other, and this is represented by Figure 1 for the copper(II)−ChPrPAc119−127NH_2 system.

It is clear from Figure 1 and Table 1 that, in all systems, complex formation starts around pH 4 with the formation of the doubly protonated species $[CuH_2L]^{4+}$. Taking into account the number of protonation sites of the ligands and the spectral parameters in Table 2, we expect monodentate binding of the His(imidazole) residue in this species. Any CD activity cannot be observed below pH 5.5, providing further support that imidazole-N donor atoms are the primary binding sites of the ligands. The stability constants of the species $[CuHL]^{3+}$ can be calculated only in the copper(II)−HuPrPAc-106−114-NH_2 system, but the concentration of the complex is rather low even in this case, and its formation largely overlaps with $[CuL]^{2+}$ and $[CuH_2L]^{4+}$. The pK_{-1} values (Table 1) are close to those of a 2N complex, with the metal ion coordinated by the imidazole and one amide-nitrogen donor atom ($[CuHL]^{3+}$= $[Cu(H_{-1}L)H_2]^{3+}$). In the case of ChPrPAc119−127NH_2 and ScrAc106−126NH_2, the 2N complex cannot be identified at all, and the formation of the species $[CuL]^{2+}$ from $[CuH_2L]^{4+}$ takes place in one step, in a cooperative manner. Thus, the pK_{-n} values of the successive deprotonation of the amide functions cannot be calculated for these ligands, only an average of the first two deprotonation (pK_{-12}) can be given. The unusual trend of pK_{-1} and pK_{-2} values, however, reveals that the deprotonation of first two amide functions is cooperative for all ligands. In these three copper(II)−peptide systems, this reaction is accompanied with a significant blue shift of the absorption spectra, supporting the deprotonation and coordination of two amide functions. The His and Lys amide groups are involved in the binding of copper to the HuPrPAc106−114NH_2 and ChPrPAc119−127NH_2 peptides, whereas the His and Gly residues bind the metal ion in the case of complex ScrAc106−126NH_2. The $N_{im} \rightarrow Cu^{2+}$ (λ_{max} = 240−260 nm) and $N^- \rightarrow Cu^{2+}$ (λ_{max} = 330−350) CD bands clearly indicate that $[CuL]^{2+}$ is a 3N complex with [N_{im}, 2 × N(amide)$^-$] binding sites, while the lysyl ϵ-ammonium groups are still protonated. In fact, the stoichiometry

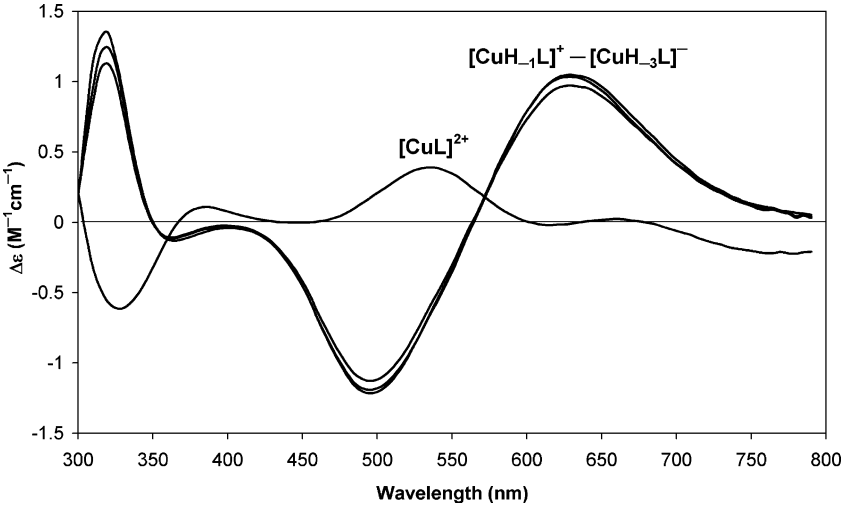

Figure 2. Molar CD spectra of the species formed in the copper(II)−HuPrPAc106−114NH_2 system. (metal-to-ligand ratio 1:1; HuPrPAc106−114NH_2 = L). The spectra are calculated using the computational program PSEQUAD.

Scheme 1. Proposed Structure of $[CuL]^{2+} = [Cu(H_{-2}L)H_2]^{2+}$

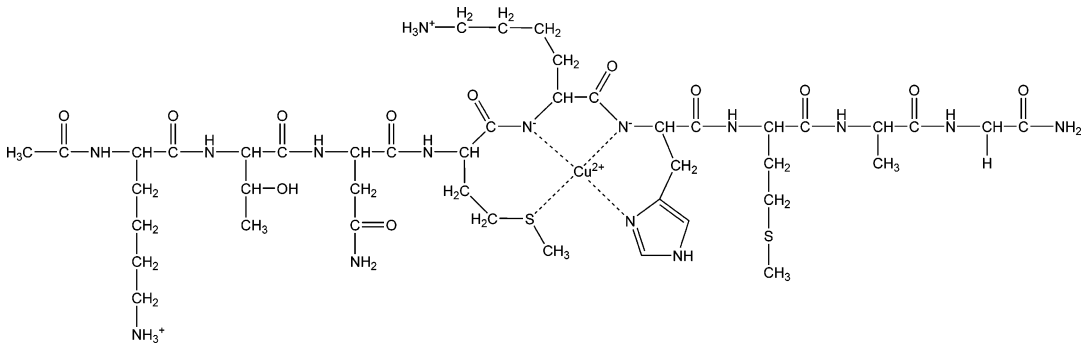

of the species is $[CuL] = [Cu(H_{-2}L)H_2]^{2+}$. The $g_{||}$ and $A_{||}$ values (Table 2) are similar to those reported for analogous species of the copper(II) complex with the prion octarepeat (see Supporting Information Figures S1 and S2).[41] These data support previous findings that the coordination of the imidazole nitrogen atoms promotes the deprotonation and coordination of the amide functions.[44] In the case of the octarepeat segments of the prion protein, the deprotonation takes place toward the C-termini in the form of a seven-membered chelate, and it is explained by the presence of proline residue.[41,42] The nonapeptides HuPrPAc106−114NH_2 and ChPrPAc119−127NH_2, however, do not contain proline, thus the formation of the six-membered chelate toward the N-terminus is more probable. It is obvious from the Tables 1 and 2 that both the equilibrium and spectral parameters of the Cu(II)−HuPrPAc106−114NH_2 and Cu(II)−ChPrPAc119−127NH_2 systems are very similar, but a slight difference between the CD spectra can be observed in the pH range from 6 to 8. The CD spectra of the systems were recorded as a function of pH, and the individual spectrum of each complex species (Figure 2) was calculated with the general computational program, PSEQUAD.[38]

The charge-transfer transitions from the copper(II)−thioether interactions generally have been found in the 320−400 nm range of the UV−vis spectra;[45−47] in the case of the Cu(II)−HuPrPAc106−114NH_2 system, a weak positive Cotton effect was observed at $\lambda = 385$ nm, and the intensity of this band was a function of the concentration of the species $[CuL]^{2+}$. This spectroscopic result shows that a weak equatorial binding of the thioether donor atom of a Met residue is involved in the binding, as shown in Scheme 1.

Previous studies on the copper(II) complexes of the neurotoxic peptide PrP106−126 resulted in differing conclusions regarding the binding ability of thioether residues: Met109 residues, Met112 residues, or both were suggested as important bridging ligands,[23] while neither the methionyl thioether nor lysyl amino groups were suggested as metal binding sites.[26] Now, our studies reveal that thioether binding occurs in a pH-dependent manner. Namely, the thioether residue occupies the fourth coordination site of the metal ion in the 3N-coordinated complex. It is, however, a weak interaction and is not able to prevent the deprotonation and metal ion coordination of the subsequent amide residues. The spectroscopic data also reveal that the metal ion coordination of the thioether donor group takes place only in the species $[CuL]^{2+}$ (the "3N complex") in a narrow pH range ($6 < pH < 8$).

(44) Sanna, D.; Ágoston, Cs. G.; Sóvágó, I.; Micera, G. *Polyhedron* **2001**, *20*, 937−947.

(45) Kowalik-Jankowska, T.; Várnagy, K.; Bertalan, Cs. *J. Chem. Res. (S)* **1993**, 172−173.

(46) Várnagy, K.; Bóka, B.; Sóvágó, I.; Sanna, D.; Marras, P.; Micera, G. *Inorg. Chim. Acta* **1998**, *275*−*276*, 440−446.

(47) Õsz, K.; Bóka, B.; Várnagy, K.; Sóvágó, I.; Kurtán, T.; Antus, S. *Polyhedron* **2002**, *21*, 2149−2159.

Table 3. Stability Constants and Spectroscopic Parameters of the Copper(II) Complexes with the Chicken and Human Tetrapeptide Fragments

	ChPrPAc122−125NH$_2$[a]			
	logβ	UV−vis λ_{max} (ϵ) [nm (dm^{3}mol^{-1}cm^{-1})]	CD λ_{max} ($\Delta\epsilon$) [nm (dm^{3}mol^{-1}cm^{-1})]	EPR $g_{\|\|}/A_{\|\|}$ (10^{-4}cm^{-1})
[CuHL]	13.88(6)			2.373/133
[CuL]	7.38(11)			
[CuH$_{-1}$L]	2.02(3)	606 (98)	605 (−0.35) 510 (+0.40) 345 (−1.31) 243 (+12.3)	2.228/165
[CuH$_{-2}$L]	−6.50(4)	528 (134)	650 (+1.00) 500 (−1.33) 360 (−0.17) 320 (+1.10) 290 (−0.10) 260 (+4.49) 220 (+23.9)	2.195/195
[CuH$_{-3}$L]	16.69(4)	525 (142)	655 (+1.27) 503 (−1.84) 355 (−0.16) 320 (+0.65) 290 (−0.86) 260 (+4.82) 222 (+29.9)	2.195/195

	HuPrPAc109−112NH$_2$[b]			
	logβ	UV−vis λ_{max} (ϵ) [nm (dm^{3}mol^{-1}cm^{-1})]	CD λ_{max} ($\Delta\epsilon$) [nm (dm^{3}mol^{-1}cm^{-1})]	EPR $g_{\|\|}/A_{\|\|}$ (10^{-4}cm^{-1})
[CuHL]	13.98(11)			2.370/133
[CuL]	−			
[CuH$_{-1}$L]	2.70(5)	629 (123)	660 (+0.15) 530 (+0.33) 380 (+0.16) 325 (−1.27) 248 (+7.56) 218 (−0.75)	2.231/172
[CuH$_{-2}$L]	−6.26(9) [c][CuH$_{-2}$L]$_{3N}$: −6.78(9) [d][CuH$_{-2}$L]$_{4N}$: −6.41(9)		[c][CuH$_{-2}$L]$_{3N}$:as for [CuH$_{-1}$L] [d][CuH$_{-2}$L]$_{4N}$:as for [CuH$_{-3}$L]	
[CuH$_{-3}$L]	−16.32(9)	521 (127)	652 (+0.92) 494 (−1.56) 354 (−0.17) 316 (+0.74) 289 (−0.81) 256 (+4.80) 229 (−2.93)	2.195/194

[a] pK(His): 6.29(3). pK(Lys): 10.28(2). pK_{-12}: 5.93. pK_{-3}: 8.52. [b] pK(His): 6.22(1). pK(Lys): 10.28(1). pK_{-12}: 5.64. pK_{-3}: 8.96. [c] [CuH$_{-2}$L]$_{3N}$: 3N complex with deprotonated lysyl's ϵ-amino group. [d] [CuH$_{-2}$L]$_{4N}$: 4N complex with protonated lysyl's ϵ-amino group.

The comparison between the data obtained for the HuPrPAc106−114NH$_2$ metal binding with those concerning the synthesized tetrapeptide fragments, namely ChPrPAc122−125NH$_2$ and HuPrPAc109−112NH$_2$, is used to unambiguously determine the metal binding site. The data obtained from the potentiometric, UV−vis, and CD measurements are collected in Table 3.

For the sake of the comparison of the stability constants included in Tables 1 and 3, the tetrapeptides should be considered to contain only one lysyl residue; this results in a difference in the stoichiometry of the corresponding complex species (e.g., $[CuH_2L]^{4+}$ of the nonapeptides corresponds to $[CuHL]^{3+}$ in the tetrapeptides). Otherwise, the speciation of the nonapeptides is very similar to that of the tetrapeptides. Both the equilibrium and spectroscopic parameters of species $[CuHL]^{3+}$ of the tetrapeptides strongly indicate that it is a 1N complex with monodentate binding of histidyl residue, while the ϵ-ammonium group of lysine remains protonated at low and medium pH values. The EPR parameters of species $[CuH_{-1}L]^{+}$ correspond to those of 3N complexes,[46] with the cooperative deprotonation of two amide nitrogens and the formation of 3N complexes. The pH range for the formation of the 3N complexes of the nona- and tetrapeptides is almost the same, thus providing indirect proof that the deprotonation of the amide functions takes place on the N-terminal side of the His residues. It is also noteworthy that the CD spectra of species $[CuH_{-1}L]^{+}$ of HuPrPAc109−112NH$_2$ exhibit a weak charge-transfer band at 380 nm, which corresponds to the Cu−S(thioether) coordination. The development of this CT band is charac-

Scheme 2. Proposed Structure of $[CuH_{-1}L]^+ = [Cu(H_{-3}L)H_2]^+$

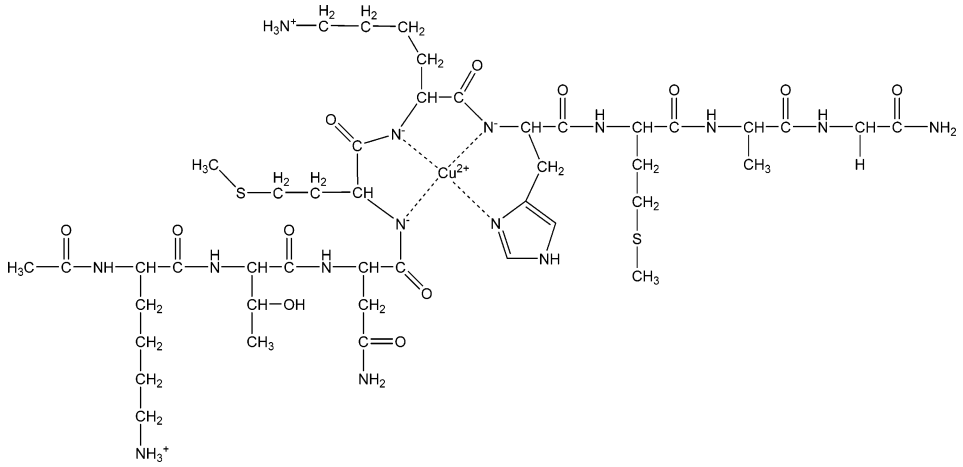

teristic only for the HuPrP peptide fragments, and its intensity changes parallel to the concentration of the 3N complex showing the involvement of Met109 in metal binding. In the case of HuPrPAc109−112NH_2, the intensity of the CT band is higher than that for the analogous nonapeptide, supporting the hypothesis that the binding of the thioether is a weak interaction and the fourth coordination site of the 3N complexes is only partially occupied by the thioether donor functions. The increase in the intensity of the CT band suggests that the ratio of the closed and open forms is higher for the tetrapeptide, in agreement with the smaller size of the molecule (Scheme 1). Similar observations have already been reported for the copper(II) complexes of tripeptides of methionine on the basis of EPR and CD measurements.[46,47]

It is clear from Tables 1 and 3 that the pK_{-12} values obtained for HuPrPAc-106−114-NH_2 and HuPrPAc-109−112-NH_2 are lower than those of the other ligands suggesting higher stability for the 3N complexes of HuPrPAc-106−114-NH_2 and HuPrPAc-109−112-NH_2. This increase in the thermodynamic stability can be easily explained by the contribution of the thioether residue of Met109 to metal binding. On the other hand, the pK_{-3} values, indicating the coordination ability of the third amide functions, are lower for peptide fragments of ChPrP, and this can be explained again by the effect of the thioether residue, which is not able to block, but slightly shifts the pH range for the binding of the third amide residues in the human peptide fragments.

A further increase in the pH results in another base-consuming process with the concomitant changes of all spectral parameters in the case of all five ligands. The spectral changes show the deprotonation and coordination of the third amide residues (Met109 and Phe122 for HuPrP and ChPrP, respectively), resulting in the formation of 4N complexes as sketched in Scheme 2. The lysyl ϵ-amino groups are still protonated in these species indicating that the real stoichiometry of the species are $[Cu(H_{-1}L)]^+ = [Cu(H_{-3}L)H_2]^+$ for the nonapeptides. Deprotonation of the lysyl side chains takes place in the same pH range as for the free ligands (pH > 9) (Table 1). These deprotonation reactions are, however, not accompanied by any spectral changes supporting the fact that the Lys residues are not metal-binding sites at any pH values. The equilibrium data provide further support for this conclusion because the protonation constants of the complexes and the free ligands (see p*K*(Cu-Lys) and p*K*(Lys) values in Table 1) are almost the same in all cases. This is in a good agreement with the most recent findings on the copper(II) complexes of the HuPrP106−126 peptides.[26] The only difference in the complex formation processes of the nonapeptides and tetrapeptides is reflected in the deprotonation of the third amide functions (pK_{-3} values) of the peptide molecules. In the case of the tetrapeptides, the metal ion coordination of the third amide functions takes place at pH values at least one log unit higher than those with the nonapeptides. This is especially true for HuPrPAc109−112NH_2, and as a consequence, the deprotonation of the third amide and the lysyl ammonium group partially overlap; the spectral parameters of the species $[CuH_{-2}L]$, therefore, can be interpreted by the assumption of two isomeric forms: (i) a 3N complex with a free lysyl amino group and (ii) a 4N complex with a protonated lysyl residue. The computer evaluation of the UV−vis and CD spectra made it possible to determine the ratio of the isomers, and values of 30% and 70% were obtained for the 3N- and 4N-coordinated isomers, respectively. In the case of ChPrPAc122−125NH_2, the deprotonations of the amide and ammonium groups are more separated (see p*K* values in Table 3), and the spectral parameters of $[CuH_{-2}L]$ correspond well to those of 4N complexes. For the interpretation of the differences in the pK_{-3} values of the nona- and tetrapeptides, it should be considered that in the case of the tetrapeptides the third amide nitrogen belongs to the acetamido group, which is much less acidic than the common peptide amide groups.[48] So, the high pK_{-3} values of the tetrapeptides provide additional proof for the assumption that the deprotonation of the amide functions goes toward the N-termini from the internal histidyl residues.

The visible absorption bands of the 3N and 4N complexes are rather unusual. Figure 3 shows the absorption spectra of all species formed in the copper(II)−HuPrPAc106−114NH_2 system, but similar data were obtained for the other peptides also. In the case of the 3N complexes, the absorption maxima are at 610 and 616 nm for the HuPrPAc106−114NH_2 and ChPrPAc119−127NH_2 peptides respectively, which cor-

(48) Sigel, H.; Martin, R. B. *Chem. Rev.* **1982**, *82*, 385−426.

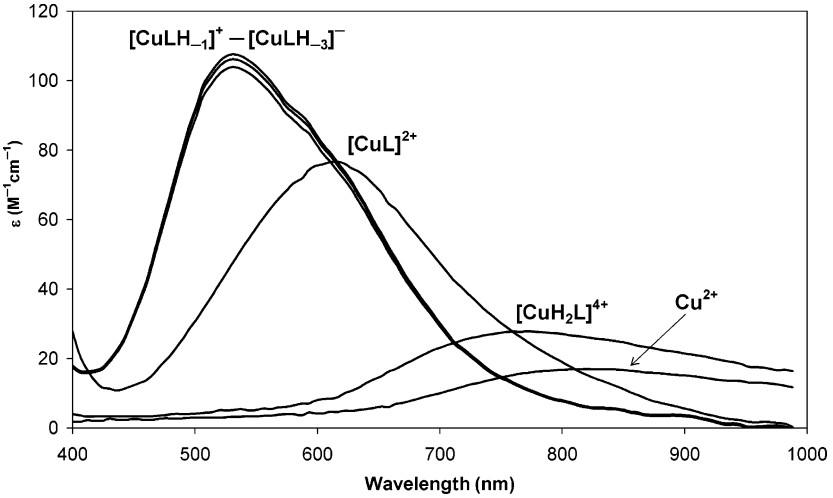

Figure 3. Molar absorption spectra of the species formed in the copper(II)−HuPrPAc106−114NH_2 system (metal-to-ligand ratio 1:1; HuPrPAc106−114NH_2 = L). The spectra are calculated using the computational program PSEQUAD.

respond to lower energies than those reported for the common 3N complexes.[49] On the other hand, the 4N complexes have wide absorption bands with well-defined shoulders on the low-energy side. All of these parameters are diagnostic of a significant distortion of the copper(II) coordination geometry in these peptide complexes.

ESI-MS of Copper(II) HuPrPAc106−114NH_2 and HuPrPAc106−126NH_2. The above-described experimental approach allowed us to unambiguously determine the copper(II) complex species existing at different pH values, as well as the amino acid residues involved in copper(II) coordination in the HuPrPAc106−114NH_2 peptide. The next step consisted of the transfer of these results to the whole HuPrPAc106−126NH_2 peptide. To do this, we resorted to ESI-MS experiments because we were not able to perform the potentiometric titrations as a result of the low solubility of the Cu(II)−HuPrPAc106−126NH_2 system at the concentrations needed to perform these measurements. In fact, recent reports on complexes of transition metal ions with peptides and other biofunctional ligands have demonstrated that the soft ionization-desorption process, occurring in electrospray ionization mass spectrometry (ESI-MS) allows the transfer of the intact species from the solution into gas phase, where they can be detected.[50,51] The high sensitivity and great accuracy in the mass assignments give direct information on metal complex formation, distinguishing the nonspecific metal adduct formation, and permit the user to obtain the stoichiometry of different species existing in dilute solutions.[52−56] First, the ESI-MS experiments were performed on the Cu(II)−HuPrPAc106−114NH_2 system to verify the correspondence of the complex species determined by the potentiometric and spectroscopic measurements with those obtained through the mass spectrometry. Then, some sets of experiments were carried out on the Cu(II)−HuPrPAc106−126NH_2 complex. The ESI-MS analysis was carried out at 1:1, 2:1, and 1:2 metal-to-ligand ratios, and the 4−11 pH range was explored.

Table 4. Assignment of the Ions Detected in the ESI-MS Spectra of Cu−HuPrPAc106−114NH_2

species	*m*/*z*
[HuPrPAc106−114NH_2]H^+	1058.3
[HuPrPAc106−114NH_2]Na^+	1080.3
[HuPrPAc106−114NH_2]H_2^{2+}	529.9
[HuPrPAc106−114NH_2]H_3^{3+}	353.5
[HuPrPAc106−114NH_2 + Cu-3H]H_2^+	1119.1 ($CuH_{-1}L$)
[HuPrPAc106−114NH_2 + Cu-3H]K^+H^+	1157.1
[HuPrPAc106−114NH_2 + Cu-2H]H_2^{2+}	560.1 (CuL)
[HuPrPAc106−114NH_2 + Cu-2H]H^+Na^+	571.1
[HuPrPAc106−114NH_2 + Cu-2H]H_3^{3+}	373.7 (only at pH5) (CuHL)
[HuPrPAc106−114NH_2 + Cu-3H]$^-$	1117.2
[HuPrPAc106−114NH_2 + Cu-4H]$^{2-}$	558.3

The ESI mass spectrum of the prion peptide fragment HuPrPAc106−114NH_2 (Table 4) shows signals of singly charged (peaks at *m*/*z* 1058.3 and 1080.3, [HuPrPAc106−114NH_2]H^+ and [HuPrPAc106−114NH_2]Na^+), doubly charged (peak at *m*/*z* 529.9, [HuPrPAc106−114NH_2] H_2^{2+}), and triply charged (peak at *m*/*z* 353.6, [HuPrPAc106−114NH_2]H_3^{3+}) species. The same signals are present in the spectra obtained throughout the pH range explored but with different relative abundance. Obviously, the peaks of single-charged species are more abundant at basic pH; conversely, the peaks of multiple-charged species are more abundant at acidic pH values.

The aqueous solution ESI mass spectrum of HuPrPAc106−114NH_2 treated with a stoichiometric amount of copper(II) sulfate is compared with the spectrum of the uncomplexed peptide fragment (Figure S3). Together with the peaks from the single-, double-, and triple-charged species of the HuPrPAc106−114NH_2 ligand, the presence of new peaks at *m*/*z* 560.1 ([HuPrPAc106−114NH_2 + Cu-2H]H_2^{2+}), 571.1 ([HuPrPAc106−114NH_2 + Cu-2H]H^+Na^+), 1119.4 ([HuPrPAc106−114NH_2 + Cu-3H]H^{2+}), and 1157 ([HuPrPAc106−114NH_2 + Cu-3H]H^+K^+) gives direct evidence of the HuPrPAc106−114NH_2/Cu complex formation. Only below pH 6, one additional peak is found at *m*/*z* 373.7 ([HuPrPAc106−114NH_2 + Cu-2H]H_3^{3+}). Spectra, obtained in the negative mode, show singly charged (peaks at *m*/*z* 1117.2,

(49) Sóvágó, I.; Sanna, D.; Dessi, A.; Várnagy, K.; Micera, G. *J. Inorg. Biochem.* **1996**, *63*, 99−117.
(50) Whittal, R. M.; Ball, H. L.; Cohen, F. E.; Burlingame, A. L.; Prusiner, S. B.; Baldwin, M. A. *Protein Sci.* **2000**, *9*, 332−343.
(51) Loo, J. A. *Int. J. Mass Spectrom.* **2001**, *204*, 113−123.

Table 5. Assignment of the Ions Detected by ESI-MS Spectra of Cu−HuPrPAc106−126NH_2

species	*m*/*z*
[HuPrPAc106−126NH_2]H^+	1953.4
[HuPrPAc106−126NH_2]H_2^{2+}	977.4
[HuPrPAc106−126NH_2]H^+Na^+	988.4
[HuPrPAc106−126NH_2]H^+K^+	995.6
[HuPrPAc106−126NH_2]H_3^{3+}	652.3
[HuPrPAc106−126NH_2]$H_2^{2+}Na^+$	659.5
[HuPrPAc106−126NH_2]$H_2^{2+}K^+$	664.7
[HuPrPAc106−126NH_2 + Cu-2H]H_2^{2+}	1007.3 (CuL)
[HuPrPAc106−126NH_2 + Cu-2H]H^+Na^+	1018.3
[HuPrPAc106−126NH_2 + Cu-2H]H^+K^+	1027.4
[HuPrPAc106−126NH_2 + Cu-2H] Na^+ K^+	1038.8
[HuPrPAc106−126NH_2 + Cu-2H]H^{3+}	672.6 (CuHL)
[HuPrPAc106−126NH_2 + Cu-2H] $H_2^{2+}Na^+$	679.6
[HuPrPAc106−126NH_2 + Cu-2H] $H_2^{2+}K^+$	687.5
[HuPrPAc106−126NH_2 + Cu-2H] $H^+Na^+K^+$	693.1
HuPrPAc106−126NH_2 + Cu-4H]$^{2-}$	1006.5 ($CuH_{-2}L$)

[HuPrPAc106−114NH_2 + Cu-3H]$^-$) and doubly charged species (at *m*/*z* 1117.2, [HuPrPAc106−114NH_2 + Cu-4H]$^{2-}$). The structural assignment of the peaks is reported in Table 4.

The ESI mass spectrum of the HuPrPAc106−126NH_2 solution (Table 5) comprises, essentially, peaks from a singly charged ion, at *m*/*z* 1953.4 ([HuPrPAc106−126NH_2]H^+), doubly charged ions at *m*/*z* 977.4 ([HuPrPAc106−126NH_2]-H_2^{2+}), *m*/*z* 988.4 ([HuPrPAc106−126NH_2]H^+Na^+), and *m*/*z* 995.6 ([HuPrPAc106−126NH_2]H^+K^+), and a triply charged ion at *m*/*z* 652.3 ([HuPrPAc106−126NH_2]H_3^{3+}).

The ESI mass spectrum of HuPrPAc106−126NH_2 in the presence of copper(II) sulfate (equimolar amount) gives direct evidence for the formation of copper(II) complexation (Figure S4). In fact, besides some signals from the still present uncomplexed peptide, the spectrum shows peaks at *m*/*z* 1007.3 (as double-charged species [HuPrPAc106−126NH_2 + Cu-2H]H_2^{2+}) and at *m*/*z* 672.6 (as triple-charged species [HuPrPAc106−126NH_2 + Cu-2H]H_3^{3+}) attributable to the copper(II)−peptide complexes. The ESI-MS spectrum, obtained in negative mode, shows signals at *m*/*z* 1006.5 (as doubly charged species [HuPrPAc106−126NH_2 + Cu-4H]$^{2-}$). The structural assignment of the peaks is reported in Table 5.

The analysis of the ESI-MS results allows the conclusion that both HuPrPAc106−114NH_2 and HuPrPAc106−126NH_2 form structurally similar copper(II) complexes, thus confirming what was previously hypothesized on the basis of visible CD, EPR, and UV−vis results.[24]

Copper(II) Influence on Peptide Conformation. The conformational features of the peptide ligands HuPrPAc106−126NH_2 and HuPrPAc106−114NH_2 have been reported elsewhere;[37] it has been demonstrated that in the absence of copper(II), these peptides adopt predominantly a random coil conformation in the whole pH range investigated.[37]

Also, the ChPrPAc119−127NH_2 and ScrHuPrPAc106−126NH_2 peptides show an unordered conformation in solution in the 4−11 pH range and in the absence of copper ions (Figure S5 and Figure S6). Conformational changes become evident when the CD spectra are recorded in the presence of the equimolar copper(II) ion. An enhancement of negative ellipticity around 220 nm, which is accompanied by the decrease of the negative dichroic band below 200 nm, is generally observed upon increasing the pH value (Figure 4). These changes are more evident in the shorter HuPrPAc106−114NH_2 fragment. Unexpectedly, the CD spectra of the ChPrPAc119−127NH_2 peptide are remarkably different, and the enhancement of a positive signal centered around 222 nm is observed as the pH increases. A comparison between the amino acid sequences of HuPrPAc106−114NH_2 and ChPrPAc119−127NH_2 indicates that Phe122 and Val125 residues substitute for the Met109 and Met112 residues, respectively, of the human sequence; thus, the signal at 222 nm could be assigned to an aromatic transition of the Phe side chain induced by complexation of the metal ion.[57] The observation of similar dichroism behavior, also in the shorter peptide fragment ChPrPAc122−125NH_2 (see Table 3), confirms the previous assignment.

The CD spectra show that copper(II) complexation brings structuring effects within the polypeptide backbone, particularly in the region involved in the binding of the metal ion. This means that the coordinated amino acid residues are forced to adopt a fixed conformation, mainly, driven by the geometrical coordination preferences of the metal ion and the stability of the chelate rings formed. This new locally defined conformation contributes, with a distinctive dichroism, to the observed spectral pattern. This is in agreement with the evidence that the CD curves of the shorter peptide sequences are affected to a greater extent by copper(II) complexation than those of the longer peptides (HuPrPAc106−126NH_2 and ScrHuPrPAc106−126NH_2).

The difference spectra obtained by subtracting the CD traces recorded without metal from those obtained in the presence of copper(II) should, in principle, give an indication of the differences in the backbone conformation caused by copper(II) complexation. Indeed, we observe that the resultant CD curves give a positive ellipticity around 195 nm and a negative signal centered around 217 nm. The ChPrPAc119−127NH_2 represents an exception: the CD curves are characterized by two positive bands at around 202 and 222 nm. Also, in this case, the positive-signed aromatic transition of the Phe side chain at 222 nm is responsible for the differring behavior.

Overall, these CD bands show the induction of an ordered structure upon metal coordination. In this regard, metal ion β-sheet-induced conformations have been proposed by other authors on the basis of similar results.[27] The CD spectra recorded for the ScrHuPrPAc106−126NH_2 in the presence of copper(II) reveal only slight conformational modifications. The difference spectra obtained show a negative ellipticity around 195 nm and a positive signal around 217 nm, which

(52) Scamporrino, E.; Vitalini, D. In *Modern Techniques for Polymer Characterization*; Pathrick, R. A., Dawkins, J. V., Eds; Wiley: New York, 1999; pp 233−266.
(53) Przybylski, M.; Glocker, M. O. *Angew. Chem., Int. Ed. Engl.* **1996**, *35*, 806−826.
(54) Wan, K. X.; Shibue, T.; Gross, M. L. *J. Am. Chem. Soc.* **2000**, *122*, 300−307.
(55) Gatlin, C. L.; Turecek, F. J. *J. Mass. Spectrom.* **2000**, *35*, 172−177.
(56) Colette, S.; Amekraz, B.; Madic, C.; Berthon, L.; Cote, G.; Moulin, C. *Inorg. Chem.* **2003**, *42*, 2215−2226.
(57) Woody, R. W.; Bunker A. K. In *Circular Dichroism and the Conformational Analysis of Biomolecules*; Fasman, G. D., Ed.; Plenum Press: New York, 1996; pp 109−157.

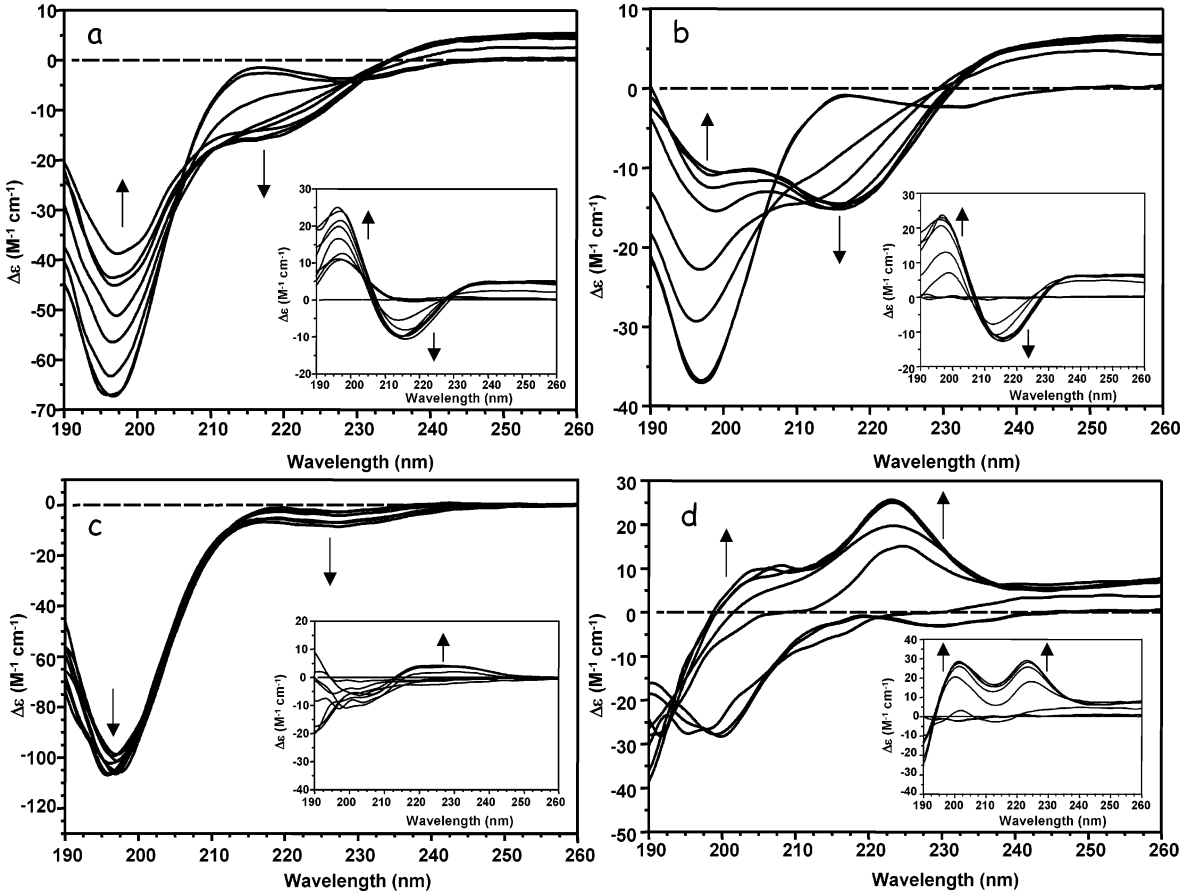

Figure 4. CD spectra of (a) Cu−HuPrPAc106−126NH_2, (b) Cu−HuPrPAc106−114NH_2, (c) Cu−ScrPrPAc106−126NH_2, and (d) Cu−ChPrPAc119−127NH_2 recorded in H_2O at different pH values and at a 1:1 metal-to-ligand ratio. The inset shows the different spectra after subtraction of the apopeptides. Arrows indicate the curve changes from pH 4 to 11.

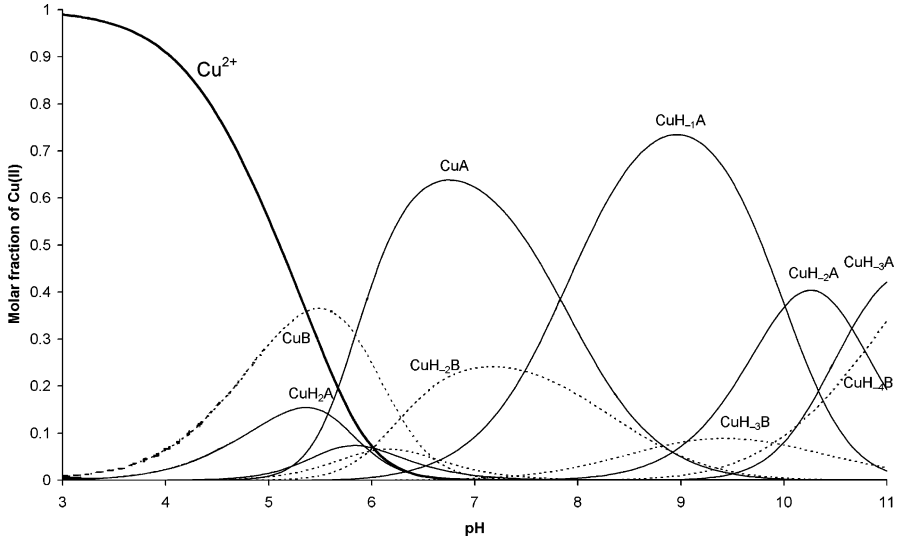

Figure 5. Species distribution diagram for the complexes formed in the copper(II)−HuPrPAc106−114NH_2 A (solid line) − and copper(II)−HuPrPAcPHGGGWGQ−NH_2 B (dotted line, data from ref 36) systems. ($[Cu^{2+}] = [A] = [B] = 4 \times 10^{-3}$ mol dm^{-3}).

are opposite to that of the HuPrPAc106−126NH_2 wild-type sequence. These results suggest that the effect of copper ion complexation may be specifically correlated with the primary structure of the peptides.

Conclusions

The PrP106−126 related peptide fragments, studied in the present paper, show higher metal-binding affinity than one single octarepeat-containing peptide fragment. This is best represented by Figure 5, where the speciation of the system Cu(II)−A−B (A = HuPrPAc106−114NH_2 and B = Ac-PHGGGWGQ-NH_2) is plotted as a function of pH. It is clear from Figure 5 that the HuPrPAc106−114NH_2 complexes dominate in the neutral and slightly basic pH ranges (e.g., [CuL] and [$CuH_{-1}L$]). Although the histidine residue is the anchoring binding site, in both the case of the octarepeat

peptide and the PrP106−126 fragment, the metal-binding patterns are significantly different. Namely, in the case of Ac-PHGGGWGQ-NH_2 the metal ion coordination starts at the His residue, but it is followed by the amide deprotonation and coordination toward the C-termini in the form of seven-membered chelates as a result of the presence of a Pro residue in the N-termini direction.[41,58,59] In the case of peptide fragments HuPrPAc106−114NH_2 and PrPAc109−112NH_2, the deprotonation takes place on the N-terminal side of the His residue in the form of six-membered chelates. Recently, preferential copper(II) coordination by His96 and His111 of the PrP protein has been claimed.[27] The nanomolar affinity of copper(II) binding to PrPAc91−115NH_2 was determined by using glycine and histidine as metal competitors at pH 7.4. Although the stoichiometry of copper(II) complexes has been obtained, the distinct species formed have not been identified.[27]

In contrast, the following claims have been made: (i) only the His96 residue is the anchoring binding site of copper(II) complexes with PrPAc90−116NH_2 and (ii) the coordination features of the PrPAc90−116NH_2 are the same as those of the copper(II) complex species with rSHaPrP90−231.[60] Both studies did not report the previous data of Cereghetti et al., showing the presence of different species in copper(II) complexes with prion protein and its fragments.[33,34] The above cited paper deals with copper complexes of rSHaPrP-90−231, PrPAc58−91NH_2, rmPrP121−231, and other mutated fragments and put into evidence not only the coexistence of different species in all pH ranges investigated but also different potential binding sites with similar EPR parameters in the full-length protein.

All of these papers[27,34,60] affirm that the copper(II) complex species formed by the prion protein fragments investigated are close to those of entire protein. However, they did not identify the species responsible for the different EPR parameters, assuming the formation of only one copper(II) complex species.

Speciation studies will be needed both to ascertain which were the main metal complex species formed by copper(II) with PrPAc91−115NH_2 at physiological pH[27] and to compare its stability constants with that of the copper(II) complex species with HuPrPAc106−114NH_2; it is now evident that the hydrophobic residues of HuPrPAc106−126NH_2 do not influence the coordination ability of the entire fragment.

The $g_{||}$ and $A_{||}$ values of the [CuL] species formed by HuPrPAc106−114NH_2 (Table 2) are close to those reported for the copper(II) complex with peptide PrPAc106−116NH_2.[60] For the latter species, it has been proposed that at least three nitrogens coordinate Cu^{2+}; in our paper the combined use of potentiometric, CD, and EPR techniques allowed us to show that, in [CuL] species, the Met109 side chain is directly involved in the copper(II) coordination, in addition to the imidazole and two deprotonated amide nitrogens (Scheme 1). This result could be of biological relevance in the light of previous studies suggesting a possible protective role, as endogenous antioxidant, for the methionine residues situated in the highly flexible amino terminal domain toward the deleterious Cu^{2+}-catalyzed oxidation that leads to PrP^C's fragmentation.[61,62]

Interestingly, the [CuL] species formed by ScrHu-PrPAc106−126NH_2 shows the same EPR parameters found for the [CuL] complex of ChPrPAc119−127NH_2 which are slightly different than those of HuPrPAc106−114NH_2 where the Met109 is involved in copper(II) coordination. Another interesting result is related to the secondary structure changes induced by metal ion complexation: these are different for HuPrPAc106−126NH_2 and ScrPrPAc106−126NH_2, showing a sequence-driven conformational variation. The different amino acid sequences have been invoked to explain the differences in the neurotoxicity exhibited by the wild-type and scrambled sequences of the PrP106−126 peptides.[8] By using PrP106−126, it has very recently been reported that, whereas the toxicity of this PrP fragment is independent of the expression level of PrP, the ScrPrP106−126 analogue is not.[63] These recently data, as well as those concerning the copper(II)-assisted toxicity of PrP106−126, were obtained by using the unblocked peptide.[19,64] This is not a good model to mimic the behavior of the fragment in the prion protein, as previously noted.[27] In fact different speciation and binding details have been reported for copper(II) complexes with PrP106−126NH_2[26] and its polar fragment, in comparison with those reported here. Although, there is not doubt about the metal complex formation, our data can give a more reliable picture of the species formed at physiological pH.

Acknowledgment. The authors thank the CNR/MTA bilateral agreement and the Hungarian National Research Fund (OTKA TS 040685, D048488, and T048352) for financial support. Ministero dell'Istruzione Università e Ricerca (MIUR) Grants 196 D.M. 1105/2002, FIRB-RBNE01ARR4, and PRIN 2003031424 are also acknowledged.

Supporting Information Available: EPR spectra recorded at different pH values, ESI positive mass spectra, and CD spectra. This material is available free of charge via the Internet at http://pubs.acs.org.

IC050754K

(58) Millhauser, G. L. *Acc. Chem. Res*. **2004**, *37*, 79−85.
(59) Bonomo, R. P.; Impellizzeri, G.; Pappalardo, G.; Rizzarelli, E.; Tabbi, G. *Chem.—Eur. J*. **2000**, *6*, 4195−4202.
(60) Burns, C. S.; Aronoff-Spencer, E.; Legname, G.; Prusiner, S. B.; Antholine, W. E.; Gerfen, G. J.; Peisach, J.; Millhauser, G. L. *Biochemistry* **2003**, *42*, 6794−6803.
(61) McMahon, H. E. M.; Mangé, A.; Nishida, N.; Creminon, C.; Casanova, D.; Lehmann, S. *J. Biol. Chem.* **2001**, *276*, 2286−2291.
(62) Requena, J. R.; Dimitrova, M. N.; Legname, G.; Teijeira, S.; Prusiner, S. B.; Levine, R. L. *Arch. Biochem. Biophys*. **2004**, *432*, 188−195.
(63) Fioriti, L.; Quaglio, E.; Massignan, T.; Colombo, L.; Stewart, R. S.; Salmona, M.; Harris, D. A.; Forloni, G.; Chiesa, R. *Mol. Cell. Neurosi.* **2005**, *28*, 165−176.
(64) Sassoon, J.; Daniels, M.; Brown, D. R. *Mol. Cell. Neurosci*. **2004**, *25*, 181−191.